Penning Ionization of $(NH_2)_2C{=}X$ (X = O, S) with He*(2^3S) Metastable Atoms. Difference of Anisotropic Interaction around N, O, and S Atoms

Naoki Kishimoto, Yukio Osada, and Koichi Ohno*

Department of Chemistry, Graduate School of Science, Tohoku University, Aramaki, Aoba-ku, Sendai 980-8578, Japan

Received: September 13, 1999

The anisotropic interaction potential energy surface around urea and thiourea ($(NH_2)_2C{=}X$, X = O,S) with the He*(2^3S) metastable atom has been studied by two-dimensional (collision-energy/electron-energy-resolved) Penning ionization electron spectroscopy and by model potential energy calculation for the molecule−Li system based on a well-known resemblance between a metastable excited He*(2^3S) atom and a ground-state Li(2^2S) atom. A different trend was found in the interaction around the C═X (X = O, S) group; an attractive interaction was found for the perpendicular direction around the C═S axis where the 3p orbital of the S atom extends, while the collinear direction along the C═O bond was found to be most attractive. A weak interaction was found around the "nitrogen lone pair" of the amino group in the conjugated systems (urea and thiourea), which is different from the general trend in previous studies that a strong attractive interaction was found around the "lone pair" of target molecules.

I. Introduction

In chemical reaction processes, it is important to investigate interaction and reaction dynamics between molecules. Especially on the anisotropic interaction potential energy surface, the movement of chemical species is not simple. Anisotropic bimolecular interaction between a metastable atom and a molecule has been studied experimentally with the use of the collisional ionization reaction (Penning ionization) with a metastable beam and collisional energy resolving technique.[1−5] Penning ionization can occur when a molecule M collides with metastable atom A* having an excitation energy larger than the lowest ionization energy of M ($M + A^* \rightarrow M^+ + A + e^-$).[6−9] In the electron exchange model[10] of the Penning ionization process, an electron in a molecular orbital (MO) having a large electron density outside the molecular surface of M is transferred to the inner-shell orbital of A*, and the excited electron in A* is ejected. Measurement of the electron kinetic energy gives Penning ionization electron spectra.[11] Because the electron distributions of individual MOs are more or less localized on a special part of a molecule, collision energy dependence of the partial ionization cross sections (CEDPICS) for various ionic states observed by the two-dimensional (collision-energy/electron-energy-resolved) Penning ionization electron spectroscopy (2D-PIES)[12] enables us to investigate the anisotropic interaction between M and A*. Negative CEDPICS shows attractive interaction, because a slower He* metastable atom can approach the reactive region effectively by an attractive force. The ionization cross section, therefore, is enhanced at lower collision energies.[1,2] On the contrary, positive CEDPICS shows repulsive interaction, because a faster He* atom can approach the reactive region effectively against the repulsive potential wall. The ionization cross section, therefore, is enhanced at higher collision energies, reflecting the exponentially increasing transition probability as a function of distance.

By observing CEDPICS, a strong attractive interaction with He*(2^3S) atoms was found for collinear direction of the C═O bond of CH_3NCO,[13] formaldehyde ($H_2C{=}O$),[14] acrolein (CH_2-$CHCH{=}O$),[14] and amides.[15] A weak interaction was found around the C═S group of CH_3NCS,[13] and the out-of-plane direction was found to be attractive around the S atom of aliphatic sulfur molecules[16] (CH_3SCH_3, CH_3SSCH_3, and C_2H_5-SH), which is different from the case of aliphatic oxygen molecules[16−18] (the in-plane direction is attractive around the O atom). In addition, it should be noted that geometry optimization was performed with ab initio calculation for H_2-CX...LiF (X = O, S),[19] and n_σ lone pair donation was found for the oxygen compound and n_π lone pair donation was found for the sulfur compound. On the other hand, a strong attractive interaction was found for the lone pair n_N orbital region of cyclopropylamine ($C_3H_5NH_2$)[20] and nitriles.[13,21,22] In addition, to obtain CEDPICS of NCCN by collision with He*(2^3S), a classical trajectory calculation was performed on the highly symmetric ($D_{\infty h}$) potential energy surface with attractive interaction around the N atoms.[23]

In this study, we have investigated the anisotropic interaction around the N, O, and S atoms with He* atoms in the conjugated system, urea and thiourea ($(NH_2)_2C{=}X$, X = O, S), by 2D-PIES and potential energy calculation. Assignments of observed bands by He I ultraviolet photoelectron spectroscopy (UPS) were made on the basis of present experiments and calculations.

II. Experimental Section

The experimental apparatus for He*(2^3S) Penning ionization electron spectroscopy was reported previously.[1−3,24] Metastable atoms of He*(2^1S, 2^3S) were produced by a discharge nozzle source with a tantalum hollow cathode. The He*(2^1S) component was quenched by a water-cooled helium discharge lamp (quench lamp). The background pressure in a reaction chamber was on the order of 10^{-7} Torr. Sample molecules were put in a sample cell set under the collision cell in the reaction chamber and heated to vaporize. He I ultraviolet photoelectron spectra (UPS) were measured by using the He I resonance photons (584 Å, 21.22 eV) produced by a discharge in pure helium gas. The kinetic energy of ejected electrons was measured by a hemi-

10.1021/jp993242y CCC: $19.00
Published on Web 01/28/2000

spherical electrostatic deflection type analyzer using an electron collection angle 90° to the incident He*(2^3S) or photon beam. The energy resolution of the electron energy analyzer was estimated to be 60 meV from the full width at half-maximum (fwhm) of the $Ar^+(^2P_{3/2})$ peak in the He I UPS. The transmission efficiency curve of the electron energy analyzer was determined by comparing our UPS data of some molecules with those by Gardner and Samson[25] and Kimura et al.[26] Calibration of the electron energy scale was made by reference to the lowest ionic state of N_2 mixed with the sample molecule in He I UPS (E_e = 5.639 eV)[27] and He* (2^3S) PIES (E_e = 4.292 eV) including a peak energy shift of 50 meV[28,29] and the difference between the metastable excitation energy and the lowest IP.

For collision-energy-resolved measurements of Penning electrons, the metastable He*(2^3S) beam was pulsed by a chopper rotating at 400 Hz, and then introduced into a reaction cell located at 504 mm downstream from the chopper disk with taking care of keeping constant sample pressure. Time dependent electron signals for each kinetic electron energy (E_e) was recorded with scanning electron energies of a 40 meV step. The two-dimensional data as functions of E_e and time t were stored in a 2 MB RAM. The resolution of the analyzer was lowered to ca. 250 meV in order to obtain higher counting rates of Penning electrons. The two-dimensional Penning ionization cross section σ (E_e, v_r) was obtained with normalization by the velocity distribution of He* $I_{He^*}(v_{He^*})$

$$\sigma(E_e,v_r) = c\{I_e(E_e,v_{He^*})/I_{He^*}(v_{He^*})\}(v_{He^*}/v_r) \quad (1)$$

$$v_r = [v_{He^*}{}^2 + 3kT/M]^{1/2} \quad (2)$$

where c is a constant, v_r is the relative velocity averaged over the velocity of the target molecule, k is the Boltzmann constant, and T and M are the gas temperature and the mass of the target molecule, respectively. Velocity distribution $I_{He^*}(v_{He^*})$ of He* beam was determined by monitoring secondary electrons emitted from the inserted stainless plate. Finally, $\sigma(E_e,v_r)$ is converted to $\sigma(E_e,E_c)$ as functions of E_e and collision energy E_c by the relation

$$E_c = \mu v_r^2/2 \quad (3)$$

where μ is the reduced mass of the system.

III. Calculations

We performed ab initio Hartree−Fock self-consistent field (SCF) calculations in order to obtain electron density maps of each MO with 6-311G** basis functions using the GAUSSIAN 94 program.[30] The geometries of neutral target molecules were selected from reported values for urea[31] and thiourea.[32] In electron density contour maps, thick solid curves indicate the repulsive molecular surface approximated by atomic spheres of van der Waals radii.[33]

Ionization potentials (IPs) were also calculated for the assignment of the photoelectron and Penning electron spectra with the outer valence Green's function (OVGF) method[34,35] using the GAUSSIAN 94 program with the 6-311G** basis function.

Interaction potential energies between He*(2^3S) and the targets for various directions were calculated on the basis of the well-known resemblance between He*(2^3S) and Li(2^2S); the shape and the total scattering cross sections of He* with He, Ar, and Kr are very similar to those of Li,[36] and the location of the interaction potential and its depth are very similar for He*-(2^3S) and Li(2^2S) with various targets.[7,37,38] Due to these findings

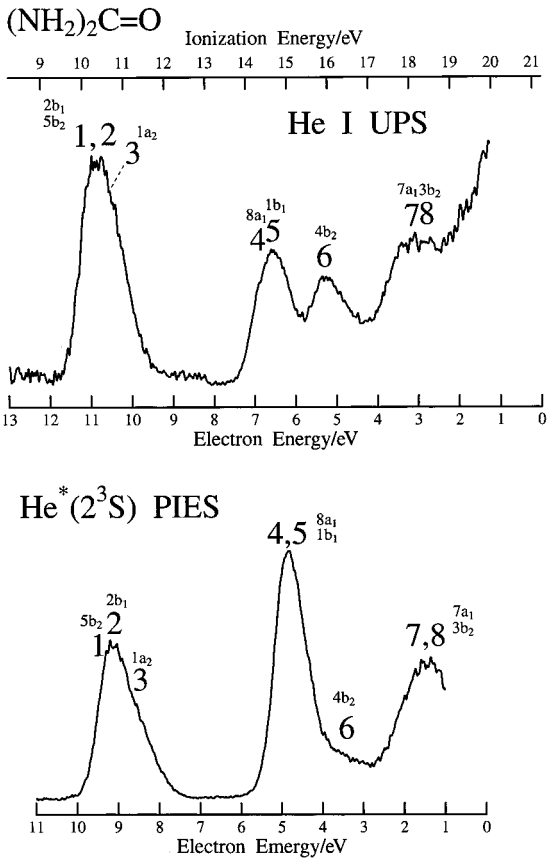

Figure 1. He I UPS and He*(2^3S) PIES of urea.

and difficulties associated with calculations for excited states, the Li atom was used in place of the He*(2^3S) atom. To taking electron correlation effects into account, we performed interaction potential energy calculations using a density functional theory (DFT) with Becke's three-parameter exchange with the Lee, Young, and Parr correlation functional (B3LYP)[39] by the GAUSSIAN 94 program with 6-311++G** basis functions for the M−Li system. In addition, interaction energy values by the unrestricted Hartree−Fock method (UHF) and second-order Møller−Plesset perturbation theory (MP2) were calculated at several points for comparison.

IV. Results

He I UPS and the He*(2^3S) Penning ionization electron spectrum (PIES) of urea and thiourea are shown in Figures 1 and 2, respectively. The electron energy scales for PIES are shifted 1.4 eV relative to those for UPS by the difference in the excitation energies between the He I photoelectron (21.22 eV) and the He*(2^3S) atom (19.82 eV).

Figures 3 and 4 show the collision-energy-resolved PIES obtained from the 2D spectra of urea and thiourea. Hot spectra at the higher collision energy (ca. 250 meV) are shown by dashed curves, and cold spectra at the lower collision energy (ca. 100 meV) are shown by solid curves.

Figures 5 and 6 show the log σ vs log E_c plots of CEDPICS in a collision energy range of 100−300 meV for urea and thiourea, respectively. The CEDPICS were obtained from the two-dimensional PIES $\sigma(E_e,E_c)$ within an appropriate range of E_e (typically the fwhm of the respective band) to avoid the effect of neighboring bands. Electron density maps are also shown in the figures in order to grasp effective access directions of He*. The calculated electron density maps for σ orbitals are shown on the molecular plane, and those for π orbitals are shown on

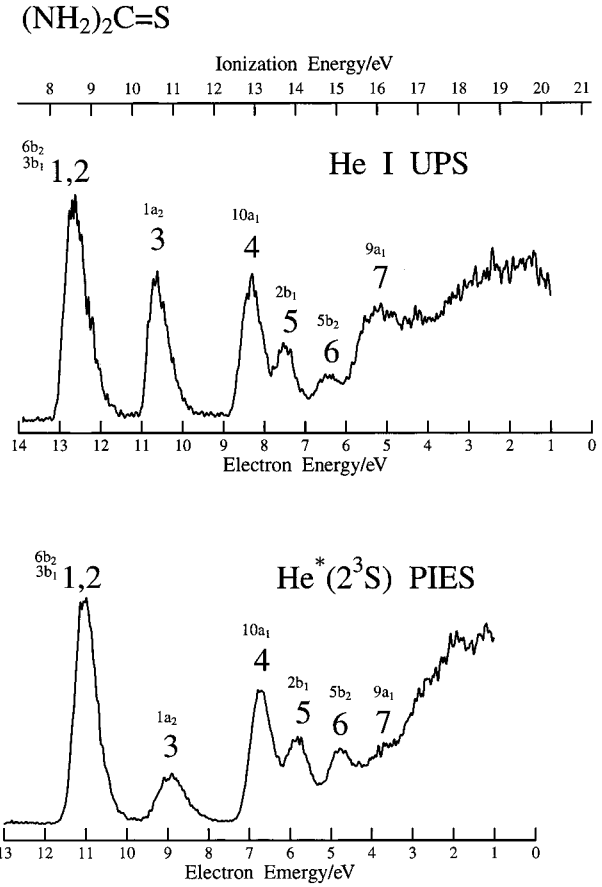

Figure 2. He I UPS and He*(2^3S) PIES of thiourea.

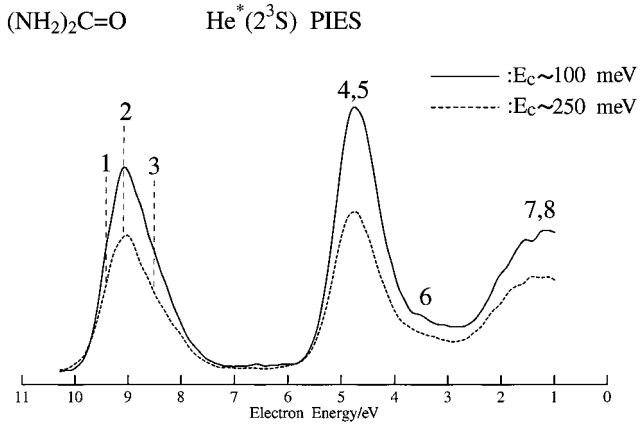

Figure 3. Collision-energy-resolved Penning ionization electron spectra of urea (solid curve at 93−107 meV, average 100 meV; dashed curve at 225−279 meV, average 250). The dotted lines show peak positions for bands 1−3.

a plane at a height of 1.70 Å (van der Waals radii of C atom) from the molecular plane.

Table 1 lists vertical IPs determined from the He I UPS and the calculated OVGF IPs. The pole strength of a respective MO was also shown in parentheses. The peak energy shifts (ΔE) in PIES measured with respect to the "nominal" energy E_0 (the difference between the metastable excitation energy and target IP) are listed. Values of the slope parameter m for the CEDPICS estimated in a collision energy range 100−300 meV by a linear least-squares method were also shown.

Potential energy curves $V(R)$ as a function of distance R and $V(\theta)$ as a function of angle C−X−Li on the molecular plane are shown for urea and thiourea in Figures 7 and 8, respectively;

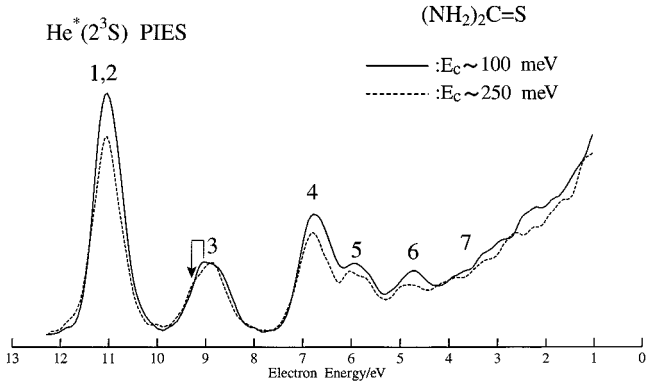

Figure 4. Collision-energy-resolved Penning ionization electron spectra of thiourea (solid curve at 93−107 meV, average 100 meV; dashed curve at 225−279 meV, average 250 meV). The arrow shows the positive energy shift of the band shoulder to larger electron energy in the hot spectrum (see text).

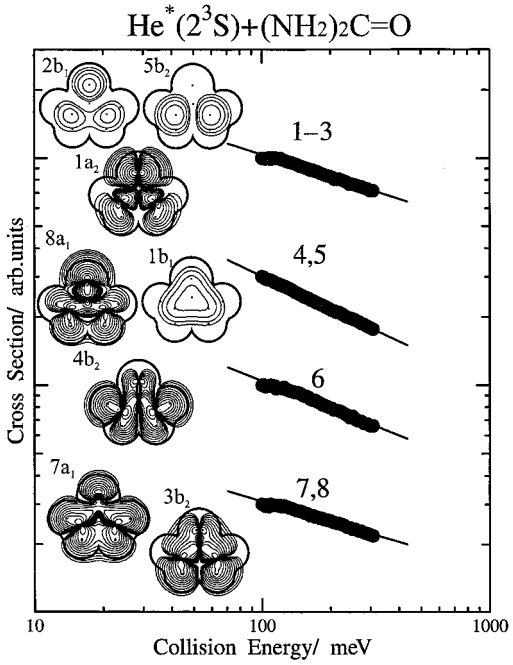

Figure 5. Collision energy dependence of the partial ionization cross sections for urea with He*(2^3S).

in (a) the distance R between Li and the molecule is measured from the molecular plane or the heteroatom, in (b) $V(\theta)$ shows potential energy curves with the X−Li distance, 1.75 Å for urea and 2.5 Å for thiourea. Model potential calculations were performed for the M−Li system with DFT. For comparison, UHF and MP2 results are also shown. Figure 9 shows potential energy curves $V(\theta,\varphi)$ by DFT calculation for thiourea−Li as a function of C−S−Li angle θ on the plane of dihedral angle φ (=30, 60, and 90°) with respect to the molecular plane with fixing S−Li distance of 2.5 Å.

V. Discussion

A. UPS and PIES of Urea. He I UPS of urea and thiourea was observed by Debies et al.[40] and Mines et al.[41] In those studies, the observed bands were assigned on the basis of semiempirical MO calculation[40] or correlation of MO level with related compounds.[41] Assignment of bands 1−3 and 4−6 of urea was, however, unresolved. In this study, we have obtained consistent results, as shown in Table 1, referring to PIES band intensity, CEDPICS, and OVGF calculation. It should be noted

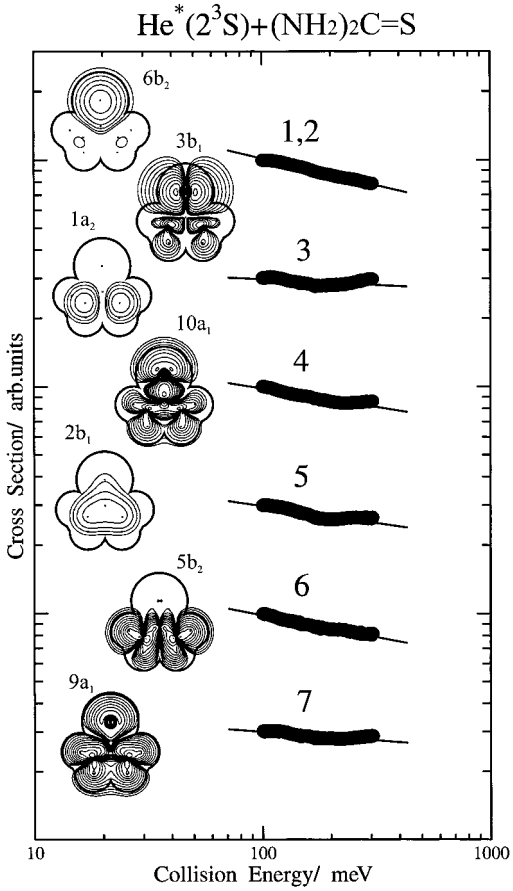

Figure 6. Collision energy dependence of the partial ionization cross sections for thiourea with He*(2^3S).

TABLE 1: Band Assignments, Ionization Potentials (IP/eV), Peak Energy Shifts (Δ*E*/eV), and Obtained Slope Parameter (*m*, See Text) for Urea and Thiourea

molecule	band	IP_{obsd}/eV	IP_{OVGF}/eV (pole strength)	orbital character	Δ*E*/eV	*m*
urea	1,2	(10.3)	9.83 (0.91)	$2b_1$ ($n_{O\perp}$)	(−0.4)	
		(10.3)	10.05 (0.91)	$5b_2$ (n_N)	(−0.1)	−0.33
	3	(10.7)	10.09 (0.92)	$1a_2$ ($n_{O//}$)	(−0.6)	
	4	(14.5)	14.52 (0.91)	$8a_1$ (σ_{CO})	(−0.5)	−0.47
	5	(14.8)	14.67 (0.90)	$1b_1$ (π_{NCO})	(−0.2)	
	6	15.95	16.57 (0.92)	$4b_2$ (σ_{NH})	(−0.4)	−0.40
	7	18.1	18.61 (0.92)	$7a_1$ (σ_{NH})	(−0.5)	−0.30
	8	18.4	18.57 (0.90)	$3b_2$ (σ_{NH})	(0.0)	
thiourea	1,2	8.6	7.79 (0.91)	$6b_2$ ($n_{S//}$)	−0.2	−0.24
		8.6	7.81 (0.91)	$3b_1$ ($n_{S\perp}$)	−0.2	
	3	10.58	10.55 (0.90)	$1a_2$ (n_N)	−0.3	−0.05
	4	12.93	12.29 (0.90)	$10a_1$ (σ_{CS})	−0.2	−0.16
	5	13.70	14.27 (0.88)	$2b_1$ (π_{NCN})	−0.3	−0.15
	6	14.81	17.01 (0.91)	$5b_2$ (σ_{NH})	−0.2	−0.19
	7	16.08	18.38 (0.85)	$9a_1$ (σ_{NH})	−0.1	−0.08

that calculated pole strengths by the OVGF method were over 0.85. This indicates that the main contribution to each ionic state is ionization from the corresponding MO.

In UPS of urea (Figure 1), the first three bands corresponding to $2b_1$ (nonbonding oxygen orbital extending in the out-of-plane direction, $n_{O\perp}$), $1a_2$ (nonbonding oxygen orbital extending in the in-plane direction, $n_{O||}$), and $5b_2$ (nonbonding nitrogen orbital extending in the out-of-plane direction, n_N) orbitals are overlapping, and the peak positions are calculated within 0.26 eV (=10.09−9.83 eV in IP). These bands show considerable negative peak energy shift in PIES with respect to IPs in UPS (Table 1), which indicates an attractive potential energy surface where the transition occurs because of the weak interaction with the ground-state helium atom for the exit channel of the reaction.

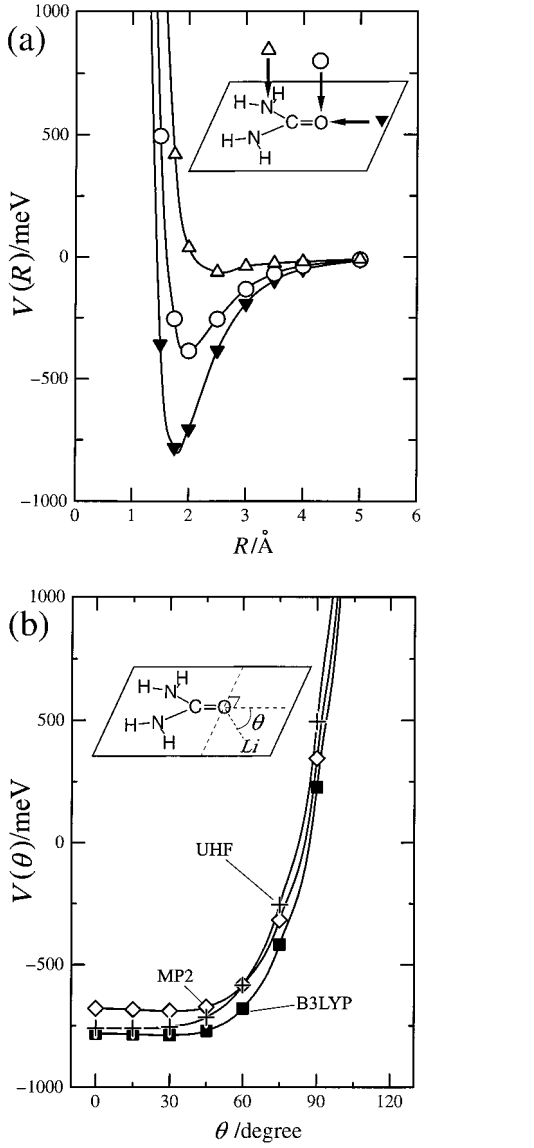

Figure 7. Model potential energy curves for urea−Li. (a) The distance *R* was measured from the N atom (△) and O atom for the out-of-plane (○) and in-plane (▼) direction. (b) The angle θ was measured from the collinear direction of the C═O group, and the distance between O and Li was kept to 1.75 Å by UHF (+), MP2 (◇), and DFT (B3LYP, ■) methods.

By decomposing overlapping bands into Gaussian type components, we can estimate the peak position and relative intensity ratios in bands 1−3 of the hot spectrum in collision-energy-resolved PIES (Figure 3) for band 1 (9.4 eV in electron energy, 5.6%), band 2 (9.1 eV, 43.2%), and band 3 (8.5 eV, 51.2%). The band intensity in PIES shows the probability of the electron-transfer process governed by mutual overlap between the orbitals of He* and M, because it is known that an electron in a molecular orbital is transferred to the inner-vacant orbital of He* and the excited electron in He* is ejected.[10] The smallest band 1 can be assigned to ionization from the $5b_2$ (n_N) orbital, because n_O bands showed similar intensities for carbonyl compounds.[42] In addition, a relatively small negative collision energy dependence of band 1 in collision-energy-resolved PIES is consistent with a weakly attractive interaction around the N atoms. Taking the potential well depth (Figure 7) into consideration as negative peak energy shift in PIES, we have roughly estimated IP values for ionization from the $2b_1$ orbital (10.3

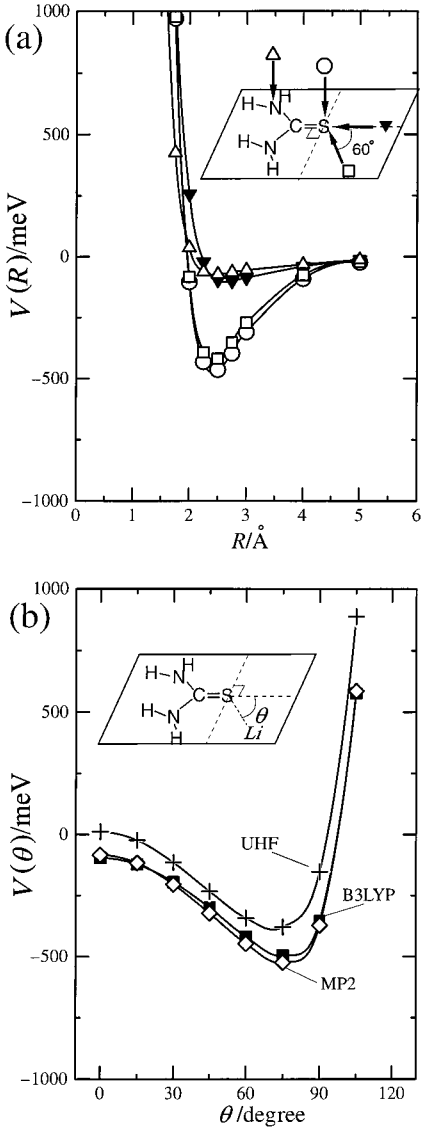

Figure 8. Model potential energy curves for thiourea−Li. (a) The distance R was measured from the N atom (△) and S atom (○) for the out-of-plane direction and in-plane direction with keeping the Li−S−C angle of 0° (▼) or 60° (□). (b) The angle θ was measured from the collinear direction of the C═S group, and the distance between S and Li was kept 2.5 Å by UHF (+), MP2 (◇), and DFT (B3LYP, ■) methods.

eV with energy shift −0.4 eV), $5b_2$ orbital (10.3 eV with energy shift −0.1 eV), and $1a_2$ orbital (10.7 eV with energy shift −0.6 eV).

The next two bands corresponding to $8a_1$ (bonding orbital extending around C═O axis, σ_{CO}) and $1b_1$ (bonding π orbital extending for the out-of-plane direction, π_{NCO}) orbitals are overlapping with an electron energy difference of 0.15 eV in the OVGF calculation. The sum of intensity for bands 1−3 is larger than that for bands 4−5 in UPS, while the intensity relationship reverses in PIES (I(1−3):I(4−5) = 1.0:1.2) by decomposing overlapping bands 4−6 into Gaussian type components. In a previous work, the band intensity was much more enhanced for the σ_{CO} band of carbonyl compounds in PIES,[42] which was ascribed to the electron distribution of the σ_{CO} orbital. In addition, the attractive interaction around the C═O group of HCHO was investigated by collision-energy-resolved Penning ionization electron spectroscopy and potential energy calculation. For urea, a strong attractive interaction was calculated for the collinear direction along the CO axis (Figure 7a), while a weak attractive interaction was calculated for the out-of-plane direction around the N atom. The enhanced intensity and strong negative collision energy dependence in collision-energy-resolved PIES (Figure 3) and CEDPICS (Figure 5) of band 4,5 are thought to be due to ionization mainly from the σ_{CO} orbital, which is consistent with the calculated results and small intensity of the π_{CO} band of HCHO[14,42] as well as the π_{NCN} band of thiourea in Figure 2. Assuming a peak energy shift from the peak position in PIES (4.8 eV in electron energy) by calculated potential well depth, we obtained the IP values for ionization from the $8a_1$ orbital (14.5 eV with energy shift −0.5 eV) and $1b_1$ orbital (14.8 eV with energy shift −0.2 eV).

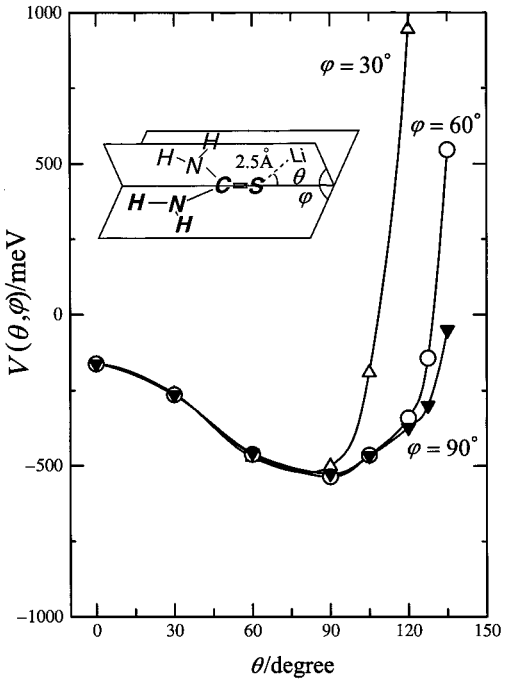

Figure 9. Model potential energy curves for thiourea−Li as a function of the angle Li−S−C (θ) with the dihedral angle φ (=30°, 60°, and 90°).

The small intensity of band 6 in PIES can be ascribed to a relatively small extension of the $4b_2$ (σ_{CH}) orbital to be ionized and the nodal plane of the orbital. Similarly, ionization from $3b_2$ is thought to result in a small intensity. The consistent assumption is, therefore, that band 7 ($7a_1$) shifts with a large negative value (−0.5 eV) and gives a relatively strong intensity due to ionization around the C═O group where the $7a_1$ orbital extends. The negative collision energy dependence of cross sections for bands 7,8 supports this assumption.

B. UPS and PIES of Thiourea. Assignment of the observed UPS bands in this study are consistent with previous studies.[40,41] Strong bands 1,2 are assigned to nonbonding sulfur orbitals extending in the out-of-plane and in-plane directions ($n_{S\perp}$, $n_{S\parallel}$), which are originated from the 3p orbital of the S atom. Contrary to the case of urea, the intensity of bands 1−3 are larger than that of bands 4−5 (I(1−3):I(4−5) = 1.7:1.0) because of the large intensity of bands 1,2. By model calculation, a strong attractive interaction was found for the perpendicular direction of the C═S axis, not around the σ_{CS} orbital region (Figure 8). The intensity of band 4 (σ_{CS}) is almost half the intensity of bands 1−2 (I(1−2):I(4) = 2.0:1.0) despite the weak attractive interaction around the C═S group, which can be ascribed to the nodal plane of $6b_2$ and $3b_1$ orbitals corresponding to bands 1,2. The large negative collision energy dependence of bands 1,2 (m = −0.24) rather than band 4 (m = −0.16) shows the

influence of attractive interaction for the perpendicular direction of the C═S group.

Band separation observed in PIES of thiourea gives information on the anisotropy of the interaction potential around the molecule. Band 3 and band 5 are assigned to $1a_2$ and $2b_1$ orbitals extending in the out-of-plane direction, respectively. A large negative peak energy shift ($\Delta E = -0.3$ eV) and negative collision energy dependence at lower collision energies (Figure 6) can be ascribed to the influence of the attractive interaction for the out-of-plane direction of the C═S group. At higher collision energies, these bands show positive collision energy dependence (slope values in Table 1 are average), as shown in Figure 6, which is due to the weak interaction on the NH_2 group. The weak attractive interactions around the "nitrogen lone pair" of urea and thiourea are unexpected and interesting, because the interaction around the lone pair of the amino group in C_3H_5-NH_2 has been known to be strongly attractive,[20] with a potential well depth of ca. 400 meV, and an attractive interaction around the "lone pair" was a general trend in previous studies.[14,16−18,20−24] It should be noted that similar unexpected weak interactions around "nitrogen lone pair" was found for amide compounds.[15]

Band 6 and band 7 are both assigned to σ_{NH} orbitals and show comparable intensities. The collision energy dependence is, however, different. The negative collision energy dependence of band 6 ($m = -0.19$) is thought to be caused by an attractive interaction for the perpendicular direction of the C═S group. This negative slope is consistent with the negative peak energy shift ($\Delta E = -0.2$ eV). The repulsive interaction around the H atoms results in a small collision energy dependence ($m = -0.08$) and peak energy shift ($\Delta E = -0.1$ eV) of band 7.

In band 3 of the collision-energy-resolved PIES (Figure 4), **a** band shoulder larger than 8.9 eV (peak position in PIES) in electron energy was observed to shift from 9.0 eV in the cold spectrum to a larger electron energy in the hot spectrum (ca. 9.2 eV), as shown in the figure by arrow. In addition, the electron energy difference of 0.2 (=9.2−9.0) eV was consistent with the collision energy difference between hot and cold spectra (0.15 eV). This shift can be ascribed to ionization on a repulsive surface, because the positive shift shows ionization near the potential wall. A similar positive shift at a higher collision energy in the hot spectrum was observed also for band 5 and band 6. These three bands are all related to ionization around the NH_2 group.

C. Slope of CEDPICS and Anisotropic Interaction Potential. Model potential energy calculations show different trends around the C═X group with the He* (or Li) atom, as mentioned above. The angular dependence of the potential energy (Figures 7b and 8b) shows a similar trend regardless of the three calculation methods (UHF, MP2, and DFT). This may show that the effect of electron correlation is not essentially important in the anisotropy of the attractive interaction in this study.

An attractive interaction was found for the collinear direction of the C═O group in the molecular plane (Figure 7), which can be ascribed to lone-pair electrons in the sp^2 hybrids on the O atom, as shown in the previous study of Penning ionization of H_2C═O.[14] In this study, we have found that the attractive interaction for the perpendicular direction around the C═S group where the 3p orbital of the S atom extends is much stronger than the collinear direction (Figures 8b and 9). We can see the attractive region spreads in a ring ($\theta = 90°$ direction) around the C═S group, as shown in Figures 8b and 9. The potential energies at θ larger than 90° are getting higher with decreasing φ, which can be ascribed to the repulsive interaction around the NH_2 group. It should be noted that a similarly attractive interaction was found in the previous studies of Penning ionization of aliphatic thioethers[16] (perpendicular direction of C−S−C plane) and ethers[17,18] (in-plane direction around the C−O−C group) as mentioned above. In addition, the perpendicular direction of the C−Cl bond (3p orbital region) was found to be more attractive with a He* atom rather than the collinear direction of the C−Cl bond in CH_2═CHCl.[43]

For atom−atom collision, when attractive interaction of R^{-s} is dominant, $\sigma(E_c)$ can be expressed by[7,44]

$$\sigma(E_c) \propto E_c^{-2/s} \tag{4}$$

If the slope parameter for the logarithm plot of CEDPICS (m) can be connected to $-2/s$, the steepness of the attractive part of potential energy curve can be derived by m. It seems that the anisotropic attractive interaction around the C═X group has a large influence on the slope of CEDPICS. The n_S bands show a larger negative dependence ($m = -0.24$) rather than the σ_{CS} band ($m = -0.16$), which is opposite to the trend seen in the n_O band ($m = -0.36 \pm 0.03$) and σ_{CO} band ($m = -0.44 \pm 0.03$) of HCHO[14] as well as band 1−3 (n_O and n_N, $m = -0.33$) and band 4−5 (σ_{CO} and π_{NCO}, $m = -0.47$) of urea. As mentioned above, in CEDPICS of thiourea (Figure 6), a bending dependence with increasing trend at higher collision energy was observed for bands 3, 4, 5, and 7, which can be ascribed to a weak interaction for the out-of-plane direction around the N atoms (band 3 and 5) or a repulsive interaction for the in-plane direction around the H atoms of two amino groups that are further from the S atom (band 4 and 7). A weak interaction around the amino group and an attractive interaction around the C═O group are consistent with a previous PIES study of amides.[45]

In connection with this study, the total electronic energy partitioning (electron kinetic energy and electron potential energy) of the energy difference between the interacting system and the noninteracting system by Tokiwa et al.[46] shows a consistent anisotropic attractive interaction and decrease of electron kinetic energy for in-plane access of a lithium atom to the O atom and out-of-plane access to the S atom of dimethyl ether or dimethyl thioether.

VI. Conclusions

By collision-energy-resolved Penning ionization electron spectroscopy and model potential energy calculation, the anisotropic interaction with a He*(2^3S) metastable atom was investigated. An attractive interaction was found for the collinear direction of the C═O axis of urea and the perpendicular direction of the C═S group. An unexpected result was obtained for both conjugated molecules; a weak interaction was found around the NH_2 group, while a strong attractive interaction was found in general around the lone pair of molecules including the nonconjugated amino compound ($C_3H_5NH_2$).[20] Observed UPS bands were assigned and several IPs for overlapping bands 1−3 and 4,5 of urea were estimated on the basis of experimental and theoretical results. Strong band intensity was observed for ionization from the σ_{CO} orbital in the Penning ionization electron spectrum of urea, while ionization from nonbonding sulfur orbitals (n_S) resulted in strong bands in PIES of thiourea.

Acknowledgment. This work has been supported by a Grant in Aid for Scientific Research from the Japanese Ministry of Education, Science, and Culture.

References and Notes

(1) Mitsuke, K.; Takami, T.; Ohno, K. *J. Chem. Phys.* **1989**, *91*, 1618.

(2) Ohno, K.; Takami, T.; Mitsuke, K.; Ishida, T. *J. Chem. Phys.* **1991**, *94*, 2675.
(3) Takami, T.; Ohno, K. *J. Chem. Phys.* **1992**, *96*, 6523.
(4) Dunlavy, D. C.; Martin, D. W.; Siska, P. E. *J. Chem. Phys.* **1990**, *93*, 5347.
(5) Dunlavy, D. C.; Siska, P. E. *J. Phys. Chem.* **1996**, *100*, 21.
(6) Penning, F. M. *Naturwissenshaften* **1927**, *15*, 818.
(7) Niehaus, A. *Adv. Chem. Phys.* **1981**, *45*, 399.
(8) Yencha, A. J. In *Electron Spectroscopy: Theory, Technique, and Applications*; Brundle, C. R., Baker, A. D., Eds.; Academic: New York, 1984; Vol. 5.
(9) Siska, P. E. *Rev. Mod. Phys.* **1993**, *65*, 337.
(10) Hotop, H.; Niehaus, A. *Z. Phys.* **1969**, *228*, 68.
(11) Čermák, V. *J. Chem. Phys.* **1966**, *44*, 3781.
(12) Ohno, K.; Yamakado, H.; Ogawa, T.; Yamata, T. *J. Chem. Phys.* **1996**, *105*, 7536.
(13) Pasinszki, T.; Yamakado, H.; Ohno, K. *J. Phys. Chem.* **1993**, *97*, 12718.
(14) Ohno, K.; Okamura, K.; Yamakado, H.; Hoshino, S.; Takami, T.; Yamauchi, M. *J. Phys. Chem.* **1995**, *99*, 14247.
(15) Kishimoto, N.; Osada, Y.; Ohno, K. To be submitted for publication.
(16) Kishimoto, N.; Yokoi, R.; Yamakado, H.; Ohno, K. *J. Phys. Chem. A* **1997**, *101*, 3284.
(17) Yamakado, H.; Yamauchi, M.; Hoshino, S.; Ohno, K. *J. Phys. Chem.* **1995**, *99*, 17093.
(18) Yamauchi, M.; Yamakado, H.; Ohno, K. *J. Phys. Chem. A* **1997**, *101*, 6184.
(19) Ammal, S. S. C.; Venuvanalingam, P.; Pal, S. *J. Chem. Phys.* **1997**, *107*, 4329.
(20) Yamakado, H.; Ogawa, T.; Ohno, K. *J. Phys. Chem. A* **1997**, *101*, 3887.
(21) Pasinszki, T.; Yamakado, H.; Ohno, K. *J. Phys. Chem.* **1995**, *99*, 14678.
(22) Kishimoto, N.; Aizawa, J.; Yamakado, H.; Ohno, K. *J. Phys. Chem. A* **1997**, *101*, 5038.
(23) Pasinszki, T.; Kishimoto, N.; Ogawa, T.; Ohno, K. *J. Phys. Chem. A*, in press.
(24) Takami, T.; Mitsuke, K.; Ohno, K. *J. Chem. Phys.* **1991**, *95*, 918.
(25) Gardner, J. L.; Samson, J. A. R. *J. Electron. Spectrosc. Relat. Phenom.* **1976**, *8*, 469.
(26) Kimura, K.; Katsumata, S.; Achiba, Y.; Yamazaki, T.; Iwata, S. *Handbook of He I Photoelectron Spectra of Fundamental Organic Molecules*; Japan Scientific: Tokyo, 1981.
(27) Turner, D. W.; Baker, C.; Baker, A. D.; Brundle, C. R. *Molecular Photoelectron Spectroscopy*; Wiley: London, 1970.
(28) Yee, D. S. C.; Stewart, W. B.; Mcdowell, C. A.; Brion, C. E. *J. Electron. Spectrosc. Relat. Phenom.* **1975**, *7*, 93.
(29) Hotop, H.; Hubler, G. *J. Electron. Spectrosc. Relat. Phenom.* **1977**, *11*, 101.
(30) Frisch, M. J.; Trucks, G. W.; Schlegel, H. B.; Gill, P. M. W.; Johnson, B. G.; Robb, M. A.; Cheeseman, J. R.; Keith, T. A.; Petersson, G. A.; Montgomery, J. A.; Raghavachari, K.; Al-Laham, M.; Zakrzewski, V. G.; Ortiz, J. V.; Foresman, J. B.; Cioslowski, J.; Stefanov, B.; Nanayakkara, A.; Challacombe, M.; Peng, C. Y.; Ayala, P. Y.; Chen, W.; Wong, M. W.; Andres, J. L.; Replogle, E. S.; Gomperts, R.; Martin, R. L.; Fox, D. J.; Binkley, J. S.; Defrees, D. J.; Baker, J.; Stewart, J. P.; Head-Gordon, M.;. Gonzales, C.; Pople, J. A. *Gaussian 94*, Revision C.3; Gaussian, Inc.: Pittsburgh, PA, 1995.
(31) Swaminathan, S.; Craven, B. M.; McMullan, R. K. *Acta Crystallogr.* **1984**, *B40*, 300.
(32) (a) Kunchuur, N. R.; Turner, M. R. *J. Chem. Soc.* **1958**, 2551. (b) Kumler, N. D.; Fohlem, G. M. *J. Am. Chem. Soc.* **1942**, *64*, 1944.
(33) Pauling, L. *The Nature of the Chemical Bond*; Cornell University: Ithaca, New York, 1960.
(34) von Niessen, W.; Schirmer, J.; Cederbaum, L. S. *Comput. Phys. Rep.* **1984**, *1*, 57.
(35) (a) Zakrewski, V. G.; Ortiz, J. V. *Int. J. Quantum Chem. Symp.* **1994**, *28*, 23. (b) Zakrzewski, V. G.; Ortiz, J. V. *Int. J. Quantum Chem.* **1995**, *53*, 583.
(36) Rothe, E. W.; Neynaber, R. H.; Trujillo, S. M. *J. Chem. Phys.* **1965**, *42*, 3310.
(37) Hotop, H. *Radiat. Res.* **1974**, *59*, 379.
(38) Haberland, H.; Lee Y. T.; Siska, P. E. *Adv. Chem. Phys.* **1981**, *45*, 487.
(39) Becke, A. D. *J. Chem. Phys.* **1993**, *7*, 5648.
(40) Debies, T.; Rabalais, J. W. *J. Electron Spectrosc. Relat. Phenom.* **1974**, *3*, 315.
(41) Mines, G. W.; Thompson, H. W. *Spectrochim. Acta* **1975**, *31A*, 137.
(42) Ohno, K.; Takano, S.; Mase, K. *J. Phys. Chem.* **1986**, *90*, 2015.
(43) Kishimoto, N.; Ohshimo, K.; Ohno, K. *J. Electron Spectrosc. Relat. Phenom.* **1999**, *104*, 145.
(44) Allison, W.; Mushulitz, E. E., Jr. *J. Electron Spectrosc. Relat. Phenom.* **1981**, *23*, 339.
(45) Keller, W.; Morgner, H.; Müller, W. A. *Mol. Phys.* **1986**, *57*, 637.
(46) Tokiwa, H.; Uchida, K.; et al. To be submitted for publication.